Supporting Information

Debye screening in single-molecule carbon nanotube field-effect transistors

Sebastian Sorgenfrei [1], Chien-yang Chiu [2], Matthew Johnston [1], Colin Nuckolls [2], Kenneth L. Shepard [1]

[1] Department of Electrical Engineering and [2] Department of Chemistry, Columbia University, New York, NY 10027

Modeling electrostatics of DNA molecule

The electrostatics of a DNA molecule tethered to a carbon nanotube is modeled using a nonlinear Poisson-Boltzmann equation for different DNA conformations relative to the nanotube. The crystal structure of a 10-mer DNA (1D68) was obtained through the Protein Data Bank [1] with charge distribution assigned through the PDB2PQR software. [2] For the carbon nanotube, we choose a zigzag (18,0) nanotube with diameter of 1.4 nm. The geometry of the three carbon spacer is estimated using ChemDraw3D (CambridgeSoft, Cambridge, MA). The nonlinear Poisson-Boltzmann equation is solved with the finite-element solver Delphi[3]. The buffer is approximated by a single salt with 0.137 M concentration and an ion radius of 0.2 nm (sodium chloride). Both the linker and carbon nanotube are assumed to be uncharged for the purpose of the electrostatic simulation, in a manner similar to other simulations.[4]

The negative charge of the DNA backbone leads to a change in potential at the carbon nanotube. We have computed the potential at the carbon nanotube surface with the single stranded probe attached and the double stranded DNA configurations as shown in Fig. 1 and then computed the potential difference between the two states. Because the DNA molecule is subject to Brownian motion, it will undergo fast rotational and translational motion, which will affect the potential at the defect. However, these motions are at times scales (<0.2μs) faster than the

bandwidth of the current device (~100μs) so the observed potential will be a distribution of all accessible configurations.

In Fig. 2b, we have computed the potential difference between the single stranded and double stranded states as a function of the rotation angle ϕ (see Fig. 2a). The potential difference is shown both precisely at the point carboxyl defect and as an average around the defect at a radius of 1.5 nm on the carbon nanotube surface (the localization roughly expected from a defect state).[5] Both potentials are relatively rotational invariant since the nanotube has a relatively large diameter.

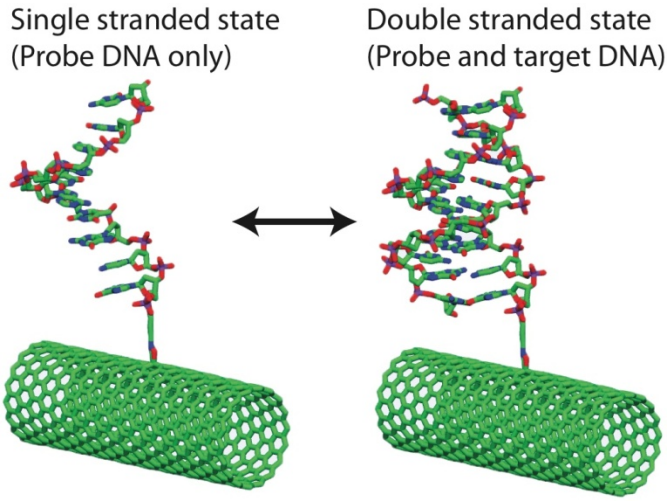

Fig. S1 Crystal structure representation of DNA attached to the carbon nanotube for both a single and double stranded configurations.

The potential difference at the surface of the carbon nanotube is plotted as a function of the tilt angle θ in Fig. S3 at a rotation angle of 90°. The defect atom is shown in the center of the figures as a dark ring and the nanotube atoms are shown as grey squares (the X axis is the direction of the length of the nanotube). As the tilt angle increases, the DNA is closer to the surface, which increases the potential difference. The potential at the defect and averaged around the defect are plotted in Fig. S4 for the different tilt angles. We attribute the change in the random telegraph

noise (RTN) amplitude in Fig. 5 to changes in the tilt angle due to electrostatic attraction of repulsion of the molecule with the surface.

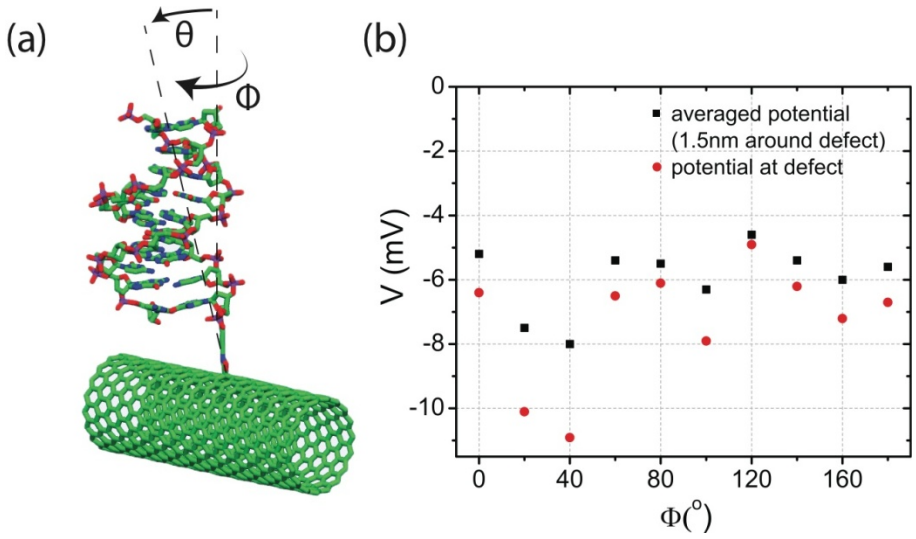

Fig. S2 (a) The configuration of the DNA molecule can change with respect to the carbon nanotube by a rotational angle ϕ and tilt angle θ. **(b)** Effect of rotational angle on the potential difference on the carbon nanotube defect.

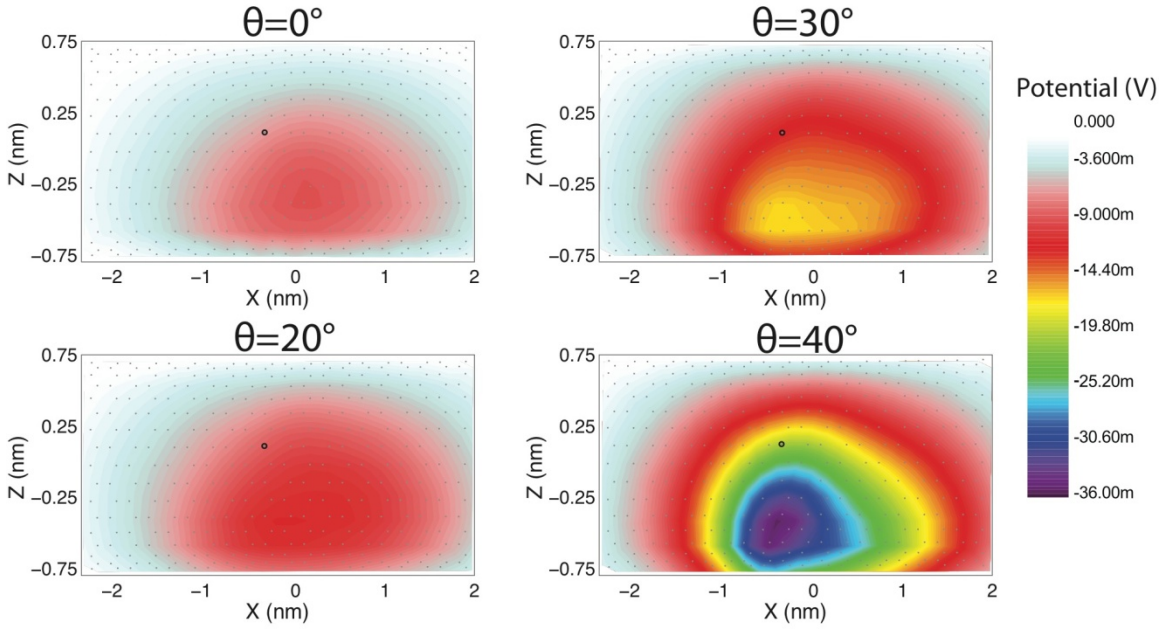

Fig. S3 Potential difference at the carbon nanotube surface for different tilt angles. The gray points are the nanotube atoms and the black ring is the position of the carboxyl defect.

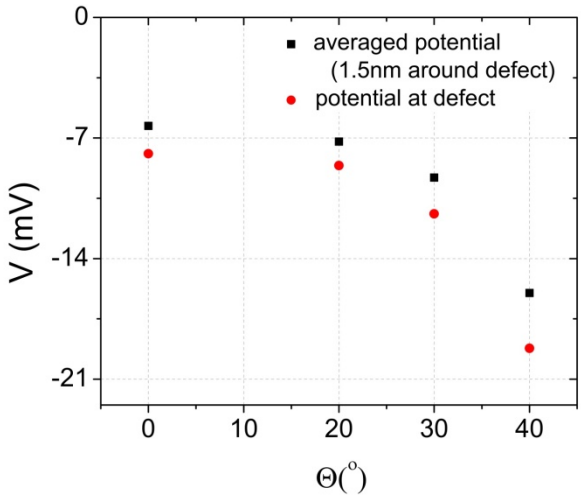

Fig. S4 Plot of potential difference at the defect and averaged around the defect for the tilt angles in Fig. S3.

Device Variability

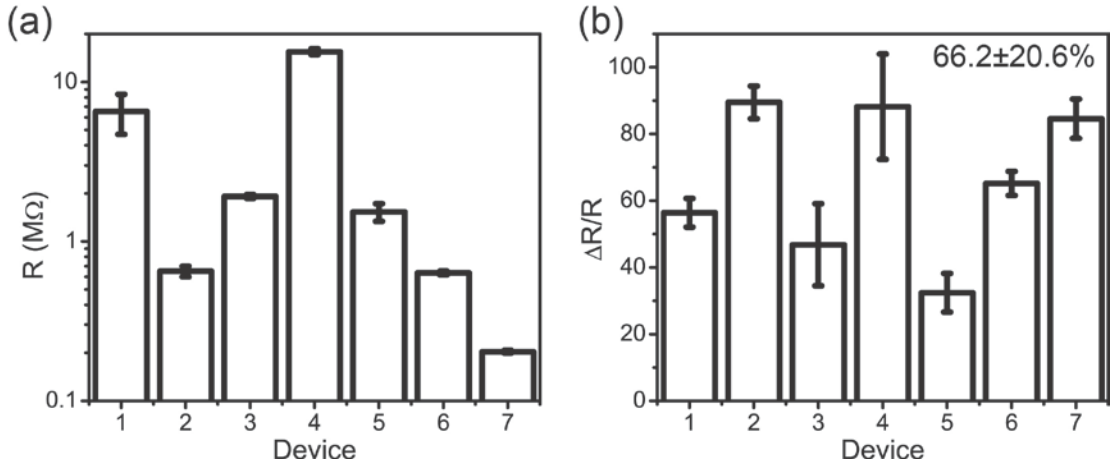

Fig. S4 (a) Standard deviation of point functionalized device resistance **(b)** and device RTN amplitude.

We have fabricated more than 7 devices, which have been functionalized with probe DNA. These devices have a wide variety of resistances spanning almost two orders of magnitude as shown in Fig. S5a. The random telegraph noise (RTN) amplitude is relatively invariant with a normalized resistance change of 66.2±20.6% as shown in Fig S5b, which is taken at 17°C or 19°C, well below the melting temperature. We attribute the variability to differences in the initial nanotube electronic properties, defect geometry , device doping and electrochemical potential.

On-chip pseudo-reference electrode

We fabricate an on-platinum electrode for controlling the solution potential. The thickness of the platinum electrode is 75 nm with a 2-nm titanium adhesion layer. As shown in Fig. S6a, the on-chip platinum electrode can be used to electrolytically gate the carbon nanotube device in 1X PBS buffer solution. The hysteresis in the gate sweep is only about 8mV at a sweep rate of 5mV/s. Because titanium is used for the source and drain electrodes of the device, the gate leakage current (shown in Fig. S6b) is below 300pA, which is more than 20 times smaller than the smallest measured device current.

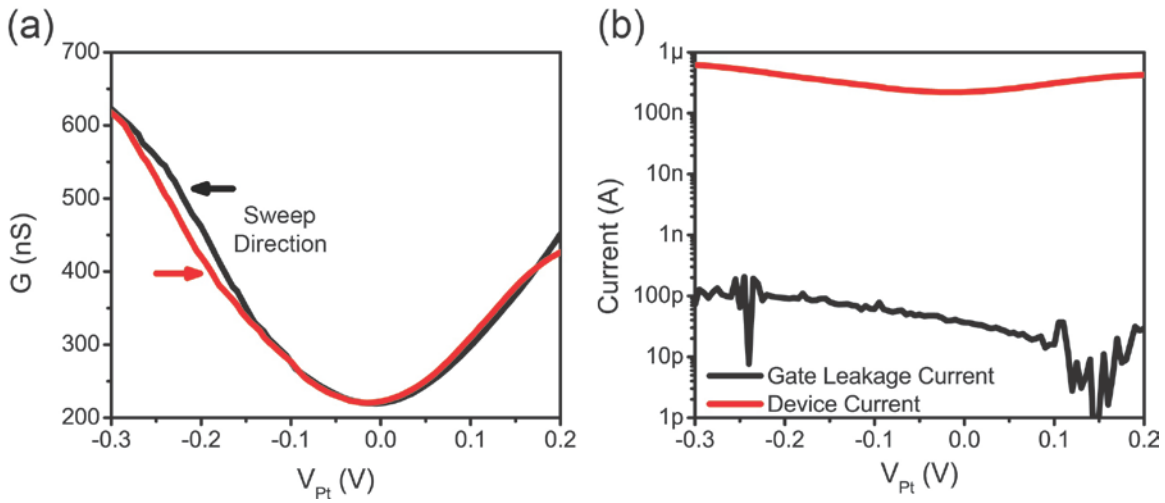

Fig. S6 (a) Hysteresis of on-chip pseudo reference electrode **(b)** Gate leakage current through 1X PBS buffer solution.

After a short transient of around 30 minutes, the open circuit potential between the Ag/AgCl/3M NaCl reference electrode (Bioanalytical Systems; 0.209V vs. NHE) and the on-chip platinum electrode is very stable as shown in Fig. S7a with a standard deviation of only 1 mV over a 90-minute observation period. The absolute value of the on-chip platinum open circuit potential is about 300mV above the potential of the platinum wire and the platinum evaporated on a glass slide (during the same evaporation step). We believe that this is the result of the annealing step in a forming gas (Hydrogen/Argon) at 340 °C. Similar to hydrogen plasma experiments[6,7], the forming gas annealing step reduces the amount of platinum oxide at the surface of the platinum electrode and therefore reduces the open circuit potential.

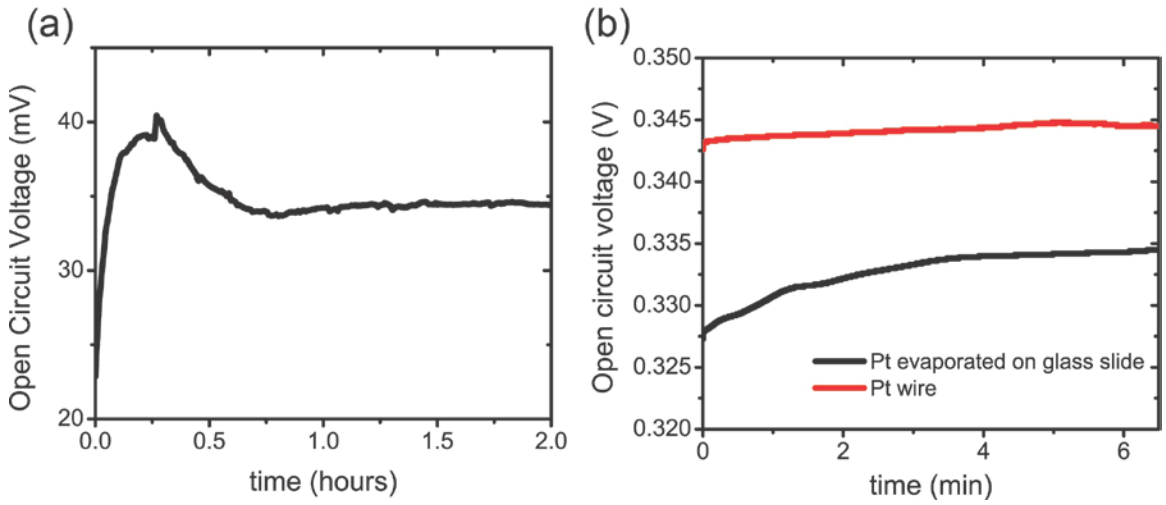

Fig. S7 (a) Open circuit voltage for on-chip platinum electrode vs. Ag/AgCl reference electrode (b) Open circuit voltage for evaporated platinum on glass and platinum wire vs. Ag/AgCl reference electrode

References

1. Cheng, J.W., Chou, S.H., Salazar, M. & Reid, B.R. SOLUTION STRUCTURE OF D(GCGTATACGC) 2. *J. Mol. Biol.* **228**, 118-137 (1992).
2. Dolinsky, T.J., Nielsen, J.E., McCammon, J.A. & Baker, N.A. PDB2PQR: an automated pipeline for the setup of Poisson-Boltzmann electrostatics calculations. *Nucleic Acids Res.* **32**, W665-W667 (2004).

3. Rocchia, W., Alexov, E. & Honig, B. Extending the applicability of the nonlinear Poisson-Boltzmann equation: Multiple dielectric constants and multivalent ions. *J. Phys. Chem. B* **105**, 6507-6514 (2001).
4. Prisbrey, L., Schneider, G. & Minot, E. Modeling the Electrostatic Signature of Single Enzyme Activity. *J. Phys. Chem. B* **114**, 3330-3333 (2010).
5. Park, H., Zhao, J.J. & Lu, J.P. Distinct properties of single-wall carbon nanotubes with monovalent sidewall additions. *Nanotechnology* **16**, 635-638 (2005).
6. Yajima, T. Electrochemical characteristics of platinum surface treated by RF plasma. *Surf Coat Tech* **112**, 80-84 (1999).
7. Li, Z.Y., Beck, P., Ohlberg, D.A.A., Stewart, D.R. & Williams, R.S. Surface properties of platinum thin films as a function of plasma treatment conditions. *Surf Sci* **529**, 410-418 (2003).